AIMS Mathematics

http://www.aimspress.com/journal/Math

AIMS Mathematics, 6(8): 8920–8948.
DOI:10.3934/math.2021518
Received: August 2020
Accepted: June 2021
Published: 15 June 2021

Research article

Correlated random walks in heterogeneous landscapes: Derivation, homogenization, and invasion fronts

Frithjof Lutscher[1,*] **and Thomas Hillen**[2]

[1] Department of Mathematics and Statistics, and Department of Biology, University of Ottawa, Ottawa, ON, K1N6N5, Canada

[2] Department of Mathematical and Statistical Sciences, University of Alberta, Edmonton, AB, T6G 2G1, Canada

* **Correspondence:** Email: frithjof.lutscher@uottawa.ca; Tel: +16135625800; Fax: +16135625776.

Abstract: Many models for the movement of particles and individuals are based on the diffusion equation, which, in turn, can be derived from an uncorrelated random walk or a position-jump process. In those models, individuals have a location but no well-defined velocity. An alternative, and sometimes more accurate, model is based on a correlated random walk or a velocity-jump process, where individuals have a well defined location and velocity. The latter approach leads to hyperbolic equations for the density of individuals, rather than parabolic equations that result from the diffusion process. Almost all previous work on correlated random walks considers a homogeneous landscape, whereas diffusion models for uncorrelated walks have been extended to spatially varying environments. In this work, we first derive the equations for a correlated random walk in a one-dimensional spatially varying environment with either smooth variation or piecewise constant variation. Then we show how to derive the so-called parabolic limit from the resulting hyperbolic equations. We develop homogenization theory for the hyperbolic equations, and show that taking the parabolic limit and homogenization are commuting actions. We illustrate our results with two examples from ecology: the persistence and spread of a population in a patchy heterogeneous landscape.

Keywords: correlated random walk; hyperbolic differential equation; multi-scale; homogenization; heterogeneous landscape; population persistence; population spread rate
Mathematics Subject Classification: 35B27, 35L40, 92D40

1. Introduction

Almost all natural landscapes exhibit spatial heterogeneity at some scale. A thorough mechanistic understanding of ecological processes, such as population persistence and spatial spread, requires some

method to deal with this heterogeneity. Homogenization is a powerful method to combine observations and measurements on a small scale to population behavior on a global scale [3]. Since the resulting multiscale analysis has been applied successfully to a variety of ecological problems [8, 14, 34, 38], homogenization of spatial ecological models has gained growing interest in quantitative ecology.

Most of the above applications are formulated as reaction-diffusion equations. They are based on a description of individual movement as an uncorrelated random walk. While quite successful and intuitive, reaction-diffusion models have also been criticized for allowing infinite propagation speeds [9]. The discussion of infinite propagation speeds in diffusion models relates to the fact that diffusion models are often derived from random walks where the individual particle speed and the turning rate are increased to infinity. It also manifests itself in the fundamental solution of the heat equation, which is positive at each point in space after arbitraily short times, even if the initial condition has compact support. Since the seminal paper by Holmes [25], modelling approaches based on correlated random walks (CRW) have received more attention. Correlated random walks are diffusive, but they do not allow for infinitely fast propagation of particles, in the sense that compact initial conditions lead to compactly supported solutions that do not expand faster than the maximum particle velocity. In one spatial dimension, they are often formulated as a system of two hyperbolic partial differential equations, and many results on existence [24], invariant regions [21], pattern formation [20, 29], chemotaxis [7, 22], epidemic spread [19], biological invasions [16, 39], and species interactions [17, 28] are known [18]. In the so-called parabolic limit, the correlated random walk approaches an uncorrelated random walk, and the associated hyperbolic equations approach the corresponding parabolic equations. However, all of these CRW models as well as their connections to the parabolic limits have only been studied in homogeneous landscapes, but see [11] for a relate model in a different context, which we discuss at the end.

In this paper, we consider the formulation and analysis, including homogenization theory, of CRW models in a one-dimensional periodically varying landscapes. We begin with smoothly varying landscapes, but the focus of the work is on "patchy" landscapes, where conditions change abruptly between different types of habitats [40]. At a boundary (or interface) between patches, the equations for the population density must be augmented by transition conditions (also called interface conditions) that describe individual movement behavior and habitat choices. We derive these conditions from the underlying random-walk model, based on ideas originally employed for uncorrelated random walks [30, 36]. Since the partial differential equations for the CRW model are hyperbolic, the transition conditions need to respect the direction of the characteristics. It turns out that the interface conditions are, in our case, discontinuous jump-conditions.

With the interface conditions in place, we apply homogenization theory to the resulting CRW models. We consider three cases. First, we homogenize a spatially inhomogeneous CRW model in a smoothly varying landscape. We compare the result to the corresponding parabolic limit and we show that the two operations of homogenizing and forming the parabolic limit commute. Next, we homogenize the patchy CRW model and compare the resulting model with the homogenization of the parabolic equations in patchy landscapes in [30, 42]. Again, we find that the parabolic limit makes the exact connection between the hyperbolic and parabolic cases. Finally, we include population dynamics such as birth and death. This allows for an analysis of classical ecological questions of species persistence conditions and invasions speeds in patchy landscapes. In particular, we compute the critical sizes of good and bad habitats such that the species can survive, we give an implicit characterization

of the invasion speed. This implicit relation cannot be solved explicitly, but homogenization provides an explicit, albeit approximate, formula. The wave speed for the homogenized reaction CRW-model can easily be obtained using a result by Hadeler [16]. We compare the explicit and implicit speeds numerically.

To keep track of the different cases considered here, we introduce the following notation. The correlated random walk with constant coefficients will be denoted as **homogeneous CRW** (see Eq (1.4)) The general model with possibly spatially dependent coefficients is simply called **CRW**, and it is the main object of our study (see Eq (2.3)). The CRW on a patchy periodic environment with jump-like transition conditions is called the **patchy CRW** (see Eq (3.1)), and if population dynamics are included, we talk about the **reaction CRW** and the **patchy reaction CRW** (see Eq (4.1)), respectively. We begin with some known results and methods for the homogeneous CRW and the homogeneous reaction CRW.

1.1. Correlated random walks in homogeneous space

In the classical approach to the one-dimensional correlated random walk, particles can move to the left or the right on the line. They do so with equal speed in both directions, so that there are exactly two velocities. To separately track particles with the two velocities, one then writes $u^{\pm}(x,t)$ to denote the densities of individuals who arrived at location x at time t by moving right (+) or left (−). During each time step (τ), particles can move a fixed distance (δ) in their given direction or change direction. In particular, right-moving particles (+) can only arrive at location x from location $x-\delta$ and left-moving particles can only arrive at x from $x+\delta$ [43].

The master equation, as derived by Zauderer and many others [17, 43], is

$$u^+(x,t+\tau) = pu^+(x-\delta,t) + (1-p)u^-(x-\delta,t), \tag{1.1}$$

$$u^-(x,t+\tau) = pu^-(x+\delta,t) + (1-p)u^+(x+\delta,t), \tag{1.2}$$

where $p = 1-\lambda\tau$ is the probability of persisting in the direction of movement and λ is the turning rate. In the limit of $\delta, \tau \to 0$ with

$$\lim_{\tau,\delta\to 0} \frac{\delta}{\tau} = \gamma, \tag{1.3}$$

we obtain the hyperbolic system of equations

$$\begin{aligned} u^+_t + \gamma u^+_x &= \lambda(u^- - u^+), \\ u^-_t - \gamma u^-_x &= \lambda(u^+ - u^-), \end{aligned} \tag{1.4}$$

where γ is the particle speed. Model (1.4) is known as the Goldstein-Kac model for correlated random walk [15, 18, 27], or, in our notation, the homogeneous CRW.

From these equations, we introduce the transformation to the total particle density $u = u^+ + u^-$ and the particle flux $v = \gamma(u^+ - u^-)$. Then we can formulate (1.4) as the equivalent hyperbolic system

$$u_t + v_x = 0, \qquad v_t + \gamma^2 u_x = -2\lambda v. \tag{1.5}$$

System (1.5) is also known as the Cattaneo system [23, 26]. If we divide the second equation of the Cattaneo system by 2λ and consider the *parabolic limit*

$$\lambda, \gamma \to \infty, \qquad 0 < \lim_{\lambda,\gamma\to\infty} \frac{\gamma^2}{2\lambda} = D < \infty, \tag{1.6}$$

we obtain Fick's law for the particle flux

$$v = -Du_x, \tag{1.7}$$

and consequently the diffusion equation

$$u_t = Du_{xx}. \tag{1.8}$$

The diffusion equation can also be obtained from a limiting process where particles (characterized by their location only), during fixed time step, jump left or right by a fixed distance [41]. Accordingly, the diffusion process is also known as a position-jump process while the CRW process is known as a velocity-jump process [34].

1.2. Reaction CRW systems in homogeneous space

Next, we include reaction into the equations. When we apply the equations to ecological processes, these reactions will model the population dynamics, i.e., births and deaths of individuals. We use general reaction terms $G^{\pm}$ and assume that population dynamics and species movement are independent stochastic processes on the same time scale. This assumption is standard, also for reaction-diffusion models, and it allows us to add the relative contributions of random walk and population kinetics into the model [17, 18, 33]. We obtain the equations

$$\begin{aligned} u^+_t + \gamma u^+_x &= \lambda(u^- - u^+) + G^+(u^+, u^-), \\ u^-_t - \gamma u^-_x &= \lambda(u^+ - u^-) + G^-(u^+, u^-). \end{aligned} \tag{1.9}$$

We call model (1.9) the homogeneous reaction CRW. A generic form for $G^{\pm}$ is

$$G^{\pm}(u^+, u^-) = \frac{m(u)}{2}u - g(u)u^{\pm}, \qquad u = u^+ + u^-, \tag{1.10}$$

where $m(u)$ is the per capita growth rate and $g(u)$ is the death rate. Unless the growth rate at low density exceeds the death rate, the population will go extinct. Hence, we shall make the assumption $m(0) > g(0)$ from hereon. The factor 1/2 indicates that newborns move in either direction with equal probability. It is useful to introduce the net kinetic term

$$f(u) := G^+(u^+, u^-) + G^-(u^+, u^-) = m(u)u - g(u)u.$$

Hadeler proved in [16] that, under certain conditions on the growth function $f(u)$, there is a critical invasion speed $0 < c_H < \gamma$, such that system (1.9) has constant-speed travelling wave solutions for all speeds in the interval $[c_H, \gamma)$. The minimum wave speed c_H can be calculated as

$$c_H = \frac{2\gamma\sqrt{F'(0)}}{1 + F'(0)}, \quad \text{where} \quad F(u) = \frac{f(u)}{2\lambda + g(u)}. \tag{1.11}$$

One set of conditions is that f satisfy $f(0) = f(1) = 0$ and $f(u) > 0$ on $(0, 1)$, and that F be concave, linearly bounded and have its maximum slope at zero. Hadeler's proof is based on comparison with the analysis of travelling fronts for a corresponding parabolic equation.

We can obtain the bound c_H as the smallest speed for which there are monotone travelling profiles in the linearized system. We linearize the above system at $u^{\pm} = 0$ and write $m_0 = m(0)$ and $g_0 = g(0)$.

We make the travelling-wave ansatz $u^{\pm}(t,x) = \phi^{\pm}(x-ct)$ with $0 < c < \gamma$. Then the above hyperbolic system turns into the ODE system

$$\begin{aligned}(\gamma - c)\dot{\phi}^{+} &= \left(\frac{m_0}{2} - g_0 - \lambda\right)\phi^{+} + \left(\frac{m_0}{2} + \lambda\right)\phi^{-}, \\ -(\gamma + c)\dot{\phi}^{-} &= \left(\frac{m_0}{2} + \lambda\right)\phi^{+} + \left(\frac{m_0}{2} - g_0 - \lambda\right)\phi^{-}.\end{aligned} \tag{1.12}$$

The matrix of this linear system is given by

$$M_H := \begin{bmatrix} \frac{A}{\gamma - c} & \frac{B}{\gamma - c} \\ \frac{-B}{\gamma + c} & \frac{-A}{\gamma + c} \end{bmatrix} \tag{1.13}$$

with $A = \frac{m_0}{2} - g_0 - \lambda$ and $B = \frac{m_0}{2} + \lambda$. For the travelling profiles to be biologically relevant, i.e. positive, the eigenvalues of this matrix M_H must be real. The eigenvalues are real if and only if

$$c \geq c_H = \frac{\gamma}{\beta}\sqrt{(\beta - \alpha)(\beta + \alpha)} = \frac{2\gamma}{m_0 + 2\lambda}\sqrt{(m_0 - g_0)(2\lambda + g_0)}. \tag{1.14}$$

In this notation, we have $F'(0) = \frac{m_0 - g_0}{2\lambda + g_0}$, so that the two expressions for c_H in (1.11) and (1.14) agree.

For completeness, we note that the situation for parabolic reaction-diffusion equations, corresponding to the uncorrelated random walk, is quite different. As is well known, the equation

$$u_t = Du_{xx} + \tilde{f}(u)$$

has constant speed traveling waves for all speeds greater than the minimum speed $c^* = 2\sqrt{D\tilde{f}'(0)}$, provided that $\tilde{f}$ is of Fisher-KPP type, i.e., $\tilde{f}(0) = \tilde{f}(1) = 0$, $\tilde{f}(u) > 0$ for $0 < u < 1$, and $\tilde{f}(u) \leq \tilde{f}'(0)u$. In particular, there is no upper limit to the speed of traveling waves [12].

2. CRW in smoothly varying landscapes

We consider a spatially-dependent CRW where parameters vary smoothly (and periodically) in space. We derive the CRW model from a master equation, consider the parabolic limit, and perform the homogenization scaling. We show that homogenizing the parabolic limit leads to the same result as taking the parabolic limit of the homogenized model.

2.1. Derivation of the spatially inhomogeneous CRW model

We generalize the derivation of the homogeneous CRW model in two aspects: we allow the turning rate to depend on space and we allow a particle to not move during a time step. We introduce the new parameter $\mu = \mu(x)$ as the probability that the particle moves away from location x. If it moves away from x, it can either persist in the direction that it had when it arrived at x or it can choose to switch direction. Then the corresponding master equations are

$$\begin{aligned}u^{+}(x, t+\tau) &= \mu(x-\delta)p(x-\delta)u^{+}(x-\delta, t) + \mu(x-\delta)\lambda(x-\delta)\tau u^{-}(x-\delta, t) \\ &\quad + (1 - \mu(x))u^{+}(x, t),\end{aligned} \tag{2.1}$$

$$\begin{aligned} u^-(x,t+\tau) &= \mu(x+\delta)p(x+\delta)u^-(x+\delta,t) + \mu(x+\delta)\lambda(x+\delta)\tau u^+(x+\delta,t) \\ &\quad +(1-\mu(x))u^-(x,t), \end{aligned} \tag{2.2}$$

where now the (conditional) persistence probability is $p(x) = 1 - \lambda(x)\tau$, and the (conditional) turning probability is $\lambda(x)\tau$. We expand the terms at $(x, t+\tau)$ as

$$u^\pm(x,t+\tau) = u^\pm + \tau u_t^\pm + O(\tau^2)$$

and the terms at $(x+\delta, t)$ as

$$u^\pm(x+\delta,t) = u^\pm + \delta u_x^\pm + O(\delta^2).$$

For functions of a single variable (e.g. μ, p), we also write the derivative in index notation (i.e. $\mu' = \mu_x$). The first two terms on the right-hand side in (2.1) expand into

$$\mu(x-\delta)p(x-\delta)u^+(x-\delta,t) = \mu p u^+ - \delta\left[\mu_x p u^+ + \mu p_x u^+ + \mu p u_x^+\right] + O(\delta^2)$$

and

$$\mu(x-\delta)\lambda(x-\delta)\tau u^-(x-\delta,t) = \tau\mu\lambda u^- + O(\delta\tau).$$

Substituting and sorting by powers of τ, δ, we obtain

$$\tau u_t^+ + O(\tau^2) = -\mu\lambda\tau(u^+ - u^-) - \delta(\mu_x u^+ + \mu u_x^+)p + O(\delta\tau, \delta^2)$$

and a similar equation for u^-. Since $p = 1 - \lambda\tau$, we have $p_x = \lambda_x\tau$, so that we can collect the corresponding terms of lower order in the O-term. Furthermore, in the limit that follows, we have $\lim_{\tau\to 0} p = 1$. Now we divide by τ and take the hyperbolic limit (1.3) to get

$$\begin{aligned} u_t^+ + \gamma(\mu(x)u^+)_x &= \mu(x)\lambda(x)(u^- - u^+), \\ u_t^- - \gamma(\mu(x)u^-)_x &= \mu(x)\lambda(x)(u^+ - u^-), \end{aligned} \tag{2.3}$$

which is the basic CRW model of this paper.

Remark 1. *The final form of the CRW model in (2.3) illustrates the importance of careful, bottom-up model derivation. We chose to modulate speed on the random walk level by introducing the function $\mu(x)$ that regulates the probability of moving. Instead, we could have started directly on the differential equation level by simply replacing the advection term $\gamma u_x^\pm$ by $(\gamma(x)u^\pm)_x$ to account for spatially dependent velocities. Our formulation $\gamma(\mu(x)u^\pm)_x$ gives us slightly more control about the effects of the particle speed γ and the motility parameter $\mu(x)$. In addition, we notice that the motility $\mu(x)$ also appears in the turning rates as the product $\mu(x)\lambda(x)$.*

2.2. Homogenization of the CRW

The notion of homogenization always relates to the appearance of different scales. Here we are interested in a local spatial scale, which we call y, and a global spatial scale, which we call x. We create these scales through a scaling parameter $\varepsilon > 0$ with $y = \frac{x}{\varepsilon}$. Now we assume that the model parameters λ and μ vary periodically on the small scale y. Without loss of generality, we may assume

that the period is equal to one. We also allow the coefficients to vary independently on the global scale x. Hence, we assume that

$$\mu(x,y), \lambda(x,y), \text{ are 1-periodic in } y.$$

Since $y = x/\varepsilon$, we can use the chain rule to replace the derivative

$$\frac{\partial}{\partial x} \to \frac{1}{\varepsilon}\frac{\partial}{\partial y} + \frac{\partial}{\partial x}. \tag{2.4}$$

Then (2.3) becomes a multiscale problem for $u^{\pm}(x,y,t)$:

$$\begin{aligned} u_t^+ + \gamma\left[\tfrac{1}{\varepsilon}(\mu(x,y)u^+)_y + (\mu(x,y)u^+)_x\right] &= \mu(x,y)\lambda(x,y)(u^- - u^+),\\ u_t^- - \gamma\left[\tfrac{1}{\varepsilon}(\mu(x,y)u^-)_y + (\mu(x,y)u^-)_x\right] &= \mu(x,y)\lambda(x,y)(u^+ - u^-). \end{aligned} \tag{2.5}$$

We make the series ansatz

$$u^{\pm}(x,y,t) = \sum_n \epsilon^n u_n^{\pm}(x,y,t),$$

where we assume that all functions $u_n^{\pm}$ are also 1-periodic in y. We substitute this expansion into (2.5) and collect orders of ε. The terms of order ϵ^{-1} are

$$(\mu(x,y)u_0^{\pm})_y = 0, \tag{2.6}$$

which we integrate over y on an interval of length 1. Since all functions and coefficients are periodic, we find that $\mu u_0^{\pm}$ must be independent of y. We define the two functions $f^{\pm}(x,t)$ via

$$u_0^{\pm}(x,y,t) = \frac{f^{\pm}(x,t)}{\mu(x,y)}. \tag{2.7}$$

The terms of order ϵ^0 are

$$u_{0,t}^{\pm} \pm \gamma\left[(\mu u_0^{\pm})_x + (\mu u_1^{\pm})_y\right] = \mu\lambda(u_0^{\mp} - u_0^{\pm}). \tag{2.8}$$

We substitute $\mu u_0^{\pm} = f^{\pm}(x,t)$ from (2.8) and solve for the terms with $u_1^{\pm}$. We obtain

$$\gamma(\mu u_1^+)_y = \lambda(f^- - f^+) - \frac{f_t^+}{\mu} - \gamma f_x^+, \tag{2.9}$$

and similar for u_1^-.

We integrate again with respect to y. Since $f^{\pm}$ are independent of y, we get

$$\gamma\mu u_1^+(x,y,t) - \gamma\mu u_1^+(x,0,t) = (f^- - f^+)\int_0^y \lambda(x,s)ds - f_t^+\int_0^y \frac{ds}{\mu(x,s)} - \gamma f_x^+ y.$$

Now we use the condition that $u^{\pm}$ and the coefficient functions are 1-periodic in y, i.e. $\gamma\mu u_1^+(x,1,t) - \gamma\mu u_1^+(x,0,t) = 0$ and

$$(f^- - f^+)\int_0^1 \lambda(x,s)ds - f_t^+\int_0^1 \frac{ds}{\mu(x,s)} - \gamma f_x^+ = 0. \tag{2.10}$$

A similar equation follows for f_t^-. We write the arithmetic and harmonic means with respect to the second variables as

$$\langle \lambda(x,\cdot)\rangle_a = \int_0^1 \lambda(x,y)dy, \quad \text{and} \quad \langle \mu(x,\cdot)\rangle_h = \left(\int_0^1 \frac{1}{\mu(x,y)}dy\right)^{-1}, \tag{2.11}$$

respectively. Then (2.10) results in the following system of hyperbolic equations for $f^\pm$:

$$\begin{aligned} f_t^+ + \gamma\langle\mu(x,\cdot)\rangle_h f_x^+ &= \langle\mu(x,\cdot)\rangle_h\langle\lambda(x,\cdot)\rangle_a(f^- - f^+),\\ f_t^- - \gamma\langle\mu(x,\cdot)\rangle_h f_x^- &= \langle\mu(x,\cdot)\rangle_h\langle\lambda(x,\cdot)\rangle_a(f^+ - f^-). \end{aligned}$$

These equations are the homogenized analogues to (2.3). It should be noted that the transport term in this hyperbolic model is not of conservation type. This is related to the fact that $u_0^\pm = f^\pm/\mu$ is a conserved quantity, while $f^\pm$ is not.

Based on the expansion above, we introduce a more formal terminology for homogenization.

> **Terminology:** *Given two spatial scales x and $y = \frac{x}{\varepsilon}$ for $\varepsilon \ll 1$, we say that model B is a homogenization of model A, if the leading-order term of a two-scale expansion of solutions of model A satisfies model B.*

In this sense we have shown:

Theorem 1. *The homogenization of*

$$\begin{aligned} u_t^+ + \gamma(\mu(x)u^+)_x &= \mu(x)\lambda(x)(u^- - u^+),\\ u_t^- - \gamma(\mu(x)u^-)_x &= \mu(x)\lambda(x)(u^+ - u^-), \end{aligned}$$

with coefficients $\mu(x,y), \lambda(x,y)$ that are 1-periodic in y, is

$$\begin{aligned} f_t^+ + \gamma\langle\mu(x,\cdot)\rangle_h f_x^+ &= \langle\mu(x,\cdot)\rangle_h\langle\lambda(x,\cdot)\rangle_a(f^- - f^+),\\ f_t^- - \gamma\langle\mu(x,\cdot)\rangle_h f_x^- &= \langle\mu(x,\cdot)\rangle_h\langle\lambda(x,\cdot)\rangle_a(f^+ - f^-). \end{aligned} \tag{2.12}$$

The zero-order term, $u_0^\pm$, in the expansion of $u^\pm$ can be obtained from the solution $f^\pm$ in (2.12) via the relation in (2.7).

2.3. The parabolic limit

We derive the parabolic limit of the homogenized equations (2.12). We use the variables $f = f^+ + f^-$ and $g = f^+ - f^-$. Then we find

$$f_t + \gamma\langle\mu(x,\cdot)\rangle_h g_x = 0, \tag{2.13}$$

$$g_t + \gamma\langle\mu(x,\cdot)\rangle_h f_x = -2\langle\mu(x,\cdot)\rangle_h\langle\lambda(x,\cdot)\rangle_a g. \tag{2.14}$$

We divide by $2\langle\mu(x,\cdot)\rangle_h\langle\lambda(x,\cdot)\rangle_a$ and take a limit in which $\lambda, \gamma \to \infty$. We consider a scaling factor $\lambda(x) = \Lambda\widehat{\lambda}(x)$ and let $\Lambda \to \infty$. In the limit

$$\lim_{\gamma,\Lambda\to\infty} \frac{\gamma^2}{2\Lambda} = \widehat{D} < \infty, \quad \text{and} \quad \frac{\widehat{D}}{\widehat{\lambda}(x)} = D(x), \tag{2.15}$$

we get

$$f_t = \langle \mu(x,\cdot)\rangle_h \left(\frac{\widehat{D}}{\langle \widehat{\lambda}(x,\cdot)\rangle_a} f_x \right)_x = \langle \mu(x,\cdot)\rangle_h (D(x) f_x)_x. \tag{2.16}$$

In particular, if μ and λ vary only on the small scale y, then we find the limiting equation

$$f_t = \frac{\langle \mu\rangle_h \widehat{D}}{\langle \widehat{\lambda}\rangle_a} f_{xx}. \tag{2.17}$$

Instead of considering the parabolic limit of the homogenized model (2.12), we can also consider the parabolic scaling of the original model (2.3). For this, we again define the total particle density $u = u^+ + u^-$ and the population flux $v = \gamma(x)\mu(x)(u^+ - u^-)$. Then we get the Cattaneo-type equations

$$u_t + v_x = 0, \qquad v_t + \gamma^2 \mu(x)(\mu(x)u)_x = -2\mu(x)\lambda(x)v.$$

As above, we divide the second equation by $2\mu(x)\lambda(x)$ and write

$$\frac{1}{2\mu(x)\lambda(x)} v_t + \frac{\gamma^2}{2\lambda(x)} (\mu(x)u)_x = -v.$$

In the limit (2.15), we obtain the diffusion equation

$$u_t = [D(x)(\mu(x)u)_x]_x. \tag{2.18}$$

By the change of variable $w(x,t) = \mu(x)u(x,t)$, we find an equivalent formulation as

$$w_t = \mu(x)(D(x)w_x)_x. \tag{2.19}$$

In this form, the equation is more amenable to some analysis. In particular, we can apply Othmer's method of homogenization for two scales x and y.

Lemma 1. *(Othmer [34]) The homogenization of*

$$U_t = \frac{1}{a(x)} \Big(a(x)d(x)U_x \Big)_x,$$

where the coefficient functions are 1-periodic on the small scale, is

$$U_{0,t} = \widetilde{d}\, U_{0,xx}, \qquad \widetilde{d} = \frac{1}{\int_0^1 a(y)dy \int_0^1 \frac{dy}{a(y)d(y)}}.$$

In our case, we assume that coefficients μ and D in (2.19) for w are 1-periodic of the small-scale variable $y = x/\epsilon$. Then we can apply Othmer's result with $a = 1/\mu$ and $d = \mu D$. We find

Lemma 2. *The homogenization of*

$$w_t = \mu(x)(D(x)w_x)_x,$$

where the coefficient functions are 1-periodic on the small scale, is

$$w_{0,t} = \widetilde{D}\, w_{0,xx}, \qquad \widetilde{D} = \frac{1}{\int_0^1 \frac{dy}{\mu(y)} \int_0^1 \frac{dy}{D(y)}} = \langle \mu\rangle_h \frac{\widehat{D}}{\int_0^1 \widehat{\lambda}(y)dy} = \frac{\langle \mu\rangle_h \widehat{D}}{\langle \widehat{\lambda}\rangle_a}. \tag{2.20}$$

Since (2.20) is identical to (2.17), the operation of homogenizing and forming a parabolic limit commute for model (2.3), at least as long as the coefficient functions only depend on the small-scale variable.

Remark 2. *There are a number of different ways in which the equation for diffusion in homogeneous space (1.8) can be extended to diffusion in heterogeneous space [5, 6, 35, 41]. Our parabolic limit (2.18) contains several of these as special cases.*

- *If D is constant then (2.18) is of Fokker-Planck type, i.e., $u_t = (d(x)u)_{xx}$, with $d(x) = D\mu(x)$, also known as ecological diffusion [41].*
- *If $D(x)$ is variable but μ is constant, then (2.18) is of Fickian type, i.e., $u_t = (d(x)u_x)_x$, with $d(x) = \mu D(x)$.*
- *If $D(x) = \mu(x)$ then (2.18) is of Wereide type, i.e, $u_t = (\sqrt{d(x)}(\sqrt{d(x)}u)_x)_x$, with $d(x) = D(x)\mu(x)$. The Wereide model can also be derived from spatially dependent speeds $\gamma(x)$ as done in [6].*
- *Finally, if we set $d(x) = D(x)\mu(x)$ and $\kappa(x) = \mu(x)/D(x)$, then (2.18) can be rewritten as*

$$u_t = \left(\sqrt{\frac{d(x)}{\kappa(x)}} \left(\sqrt{\kappa(x)d(x)}u \right)_x \right)_x ,$$

  which generalizes the Wereide model [6].

In either case, the effective diffusion coefficient is $d(x) = \mu(x)D(x)$.

3. Patchy landscapes and interfaces

In this section, we extend the fairly recent modeling approach of individual movement behaviour near sharp interfaces from uncorrelated random walks to correlated random walks. The theory for the uncorrelated walk and corresponding reaction-diffusion equation was developed by Ovaskainen and Cornell [36] and continued by Maciel and Lutscher [30]. One motivation for this approach is that continuous variation in landscape quality is difficult to parametrize and also to analyze (other than fairly abstract results). In addition, landscape ecologists typically take the view that landscapes consist of patches that are homogeneous within and different between. Hence, we have a piecewise constant landscape quality with abrupt transitions that we call interfaces. There is already a reasonably large body of empirical literature on individual behaviour and patch preference; see, e.g., references in [30]. Potts et al. [37] modelled decision making at an edge through a step selection function approach, where the decision to cross into the next habitat or stay in the original habitat depends on a non-local sensing of the environment. In their model, they could explain various forms of species abundances near interfaces that were observed in nature. Here we use a simpler approach and consider a given, fixed transition probability β.

We derive the corresponding formulas with only two patches and a single interface. Without loss of generality, we set $x = 0$ to be the location of the interface. We call the region $\{x > 0\}$ patch 1 and the region $\{x < 0\}$ patch 2; see Figure 1. Within patch i, individuals take steps of length δ_i during time intervals τ. The turning rate in patch i is $\lambda_i\tau$, the probability to remain in a given direction is $p_i = 1 - \lambda_i\tau$, and the probability to move from location x is denoted by μ_i. The speed in the limit

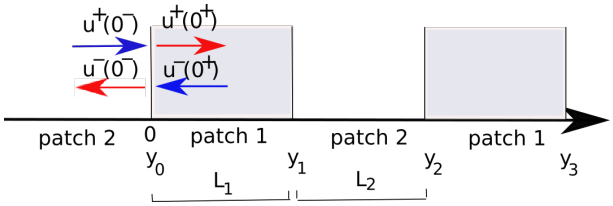

Figure 1. Sketch of the patchy one-dimensional domain.

becomes $\lim_{\tau,\delta_i\to 0}(\delta_i)/(2\tau) = \gamma_i$. Then the equations for $u^\pm$ in patch i become

$$\begin{aligned} u_t^+ + \gamma_i\mu_i u_x^+ &= \mu_i\lambda_i(u^- - u^+), \\ u_t^- - \gamma_i\mu_i u_x^- &= \mu_i\lambda_i(u^+ - u^-). \end{aligned} \tag{3.1}$$

The parameters and their meaning are summarized in Table 1. We need to prescribe the matching conditions at $x = 0$. Since the equations are hyperbolic, we can only prescribe densities along the incoming characteristics in terms of the outgoing characteristics, i.e., we need to find expressions for $u^+(0^+,t)$ and $u^-(0^-,t)$ in terms of $u^+(0^-,t)$ and $u^-(0^+,t)$. At an interface, individual behaviour is different from elsewhere since the individual can choose between two habitat types. We denote by $\beta^\pm$ the probability that an individual that arrived at the interface by moving right (left) will persist in its movement direction. The probability of moving from the interface is μ_0.

When we write the master equations, we need to be careful since the spacing in the two patches is different when $\delta_1 \neq \delta_2$. We continue to use $u^\pm$ to denote the densities. Then the probabilities that an individual who arrived by moving right (left) in an interval of length δ_1, centred at $n\delta_1$ are $u^\pm(n\delta_1,t)\delta_1 + O(\delta_1)$ with $n = 1,2,3,\ldots$. Similar notation holds for patch 2 with $u(-n\delta_2,t)\delta_2$. The interval around $x = 0$ has length $\delta_0 = (\delta_1+\delta_2)/2$. Hence, the probability that an individual is in that interval is $u^\pm(0,t)\delta_0 + O(\delta_0)$.

The relevant master equations near zero are

$$\begin{aligned} u^+(\delta_1,t+\tau)\delta_1 &= [u^+(0,t)\beta^+ + u^-(0,t)(1-\beta^-)]\mu_0\delta_0 + (1-\mu_1)u^+(\delta_1,t)\delta_1, \\ u^+(0,t+\tau)\delta_0 &= [u^+(-\delta_2,t)p_2 + u^-(-\delta_2,t)\lambda_2\tau]\mu_2\delta_2 + (1-\mu_0)u^+(0,t)\delta_0 \\ u^-(-\delta_2,t+\tau)\delta_2 &= [u^+(0,t)(1-\beta^+) + u^-(0,t)\beta^-]\mu_0\delta_0 + (1-\mu_2)u^-(-\delta_2,t)\delta_2, \\ u^-(0,t+\tau)\delta_0 &= [u^-(\delta_1,t)p_1 + u^+(\delta_1,t)\lambda_1\tau]\mu_1\delta_1 + (1-\mu_0)u^-(0,t)\delta_0. \end{aligned}$$

In the second of these equations, we expand the left-hand side as usual:

$$u^+(0,t+\tau)\delta_0 = u^+(0,t)\delta_0 + u_t^+(0,t)\tau\delta_0 + O(\tau). \tag{3.2}$$

Then we cancel like terms and rearrange the resulting equation and find

$$\mu_0 u^+(0,t)\delta_0 = [u^+(-\delta_2,t)p_2 + u^-(-\delta_2,t)\lambda_2\tau]\mu_2\delta_2 + O(\tau,\delta_0). \tag{3.3}$$

Similarly, the fourth equation gives us

$$\mu_0 u^-(0,t)\delta_0 = [u^-(\delta_1,t)p_1 + u^+(\delta_1,t)\lambda_1\tau]\mu_1\delta_1 + O(\tau,\delta_0). \tag{3.4}$$

Substituting these two expressions into the first of the master equations leads to

$$\begin{aligned}[u^+(\delta_1,t)+u_t^+(\delta_1,t)\tau]\delta_1 &= \beta^+[u^+(-\delta_2,t)p_2+u^-(-\delta_2,t)\lambda_2\tau]\mu_2\delta_2\\ &\quad+(1-\beta^-)[u^-(\delta_1,t)p_1+u^+(\delta_1,t)\lambda_1\tau]\mu_1\delta_1\\ &\quad+(1-\mu_1)u^+(\delta_1,t)\delta_1.\end{aligned}$$

We have eliminated the terms evaluated at zero. Now we can take the limit $\tau,\delta_1,\delta_2\to 0$. In the hyperbolic limit, the derivative term on the left side of the equation vanishes; hence, we omit it from here on. We can cancel one term from both sides, then divide by τ and take the limit to get the condition

$$\mu_1\gamma_1u^+(0^+,t)=\beta^+\mu_2\gamma_2u^+(0^-,t)+(1-\beta^-)\mu_1\gamma_1u^-(0^+,t), \tag{3.5}$$

which can also be written as

$$u^+(0^+,t)=\beta^+\frac{\mu_2\gamma_2}{\mu_1\gamma_1}u^+(0^-,t)+(1-\beta^-)u^-(0^+,t). \tag{3.6}$$

By symmetry considerations, the corresponding expression in the other direction is

$$u^-(0^-,t)=\beta^-\frac{\mu_1\gamma_1}{\mu_2\gamma_2}u^-(0^+,t)+(1-\beta^+)u^+(0^-,t). \tag{3.7}$$

The transition conditions (3.6) and (3.7) are illustrated in Figure 1, where the red arrows are functions of the blue arrows.

When the patch of type 1 is located to the left of the interface and the patch of type 2 on the right, then β^+ becomes the probability of a particle that moves to the left from patch 2 to patch 1 would continue to patch 1, while β^- is now the probability of continuing to the right, from a patch of type 1 to type 2. Hence, if $x=L_1$ is an interface with a patch of type 1 located at $\{x<L_1\}$ and a patch of type 2 located at $\{x>L_1\}$, we get the interface conditions:

$$\begin{aligned}u^+(L_1^+,t) &= \beta^-\tfrac{\mu_1\gamma_1}{\mu_2\gamma_2}u^+(L_1^-,t)+(1-\beta^+)u^-(L_1^+,t),\\ u^-(L_1^-,t) &= \beta^+\tfrac{\mu_2\gamma_2}{\mu_1\gamma_1}u^-(L_1^+,t)+(1-\beta^-)u^+(L_1^-,t).\end{aligned} \tag{3.8}$$

As long as the equations describe only movement and no population dynamics, the total mass of individuals should be preserved by the equations. We show that this is indeed the case with our interface conditions. We choose the simplest set-up of a single interface at $x=0$ as in the master equations, i.e., we have Eqs (3.1) with $i=1$ for $x>0$ and $i=2$ for $x<0$, and interface conditions (3.6), (3.7) at $x=0$. We assume that the densities $u^\pm$ approach zero as $|x|\to\pm\infty$. We evaluate the change in the total density

$$\begin{aligned}\frac{d}{dt}\int_{-\infty}^{\infty}(u^++u^-)(x,t)dx &= \int_{-\infty}^{0}\gamma_2\mu_2(u_x^--u_x^+)(x,t)dx+\int_0^{\infty}\gamma_1\mu_1(u_x^--u_x^+)(x,t)dx\\ &= \gamma_2\mu_2(u^--u^+)(0^-,t)-\gamma_1\mu_1(u^--u^+)(0^+,t).\end{aligned}$$

We rearrange (3.6) as

$$\mu_1\gamma_1(u^+(0^+,t)-u^-(0^+,t))=\beta^+\mu_2\gamma_2u^+(0^-,t)-\beta^-\mu_1\gamma_1u^-(0^+,t)$$

and (3.7) as

$$\mu_2\gamma_2(u^-(0^-,t)-u^+(0^-,t))=\beta^-\mu_1\gamma_1u^-(0^+,t)-\beta^+\mu_2\gamma_2u^+(0^-,t).$$

The sum of the left-hand sides of the rearranged interface conditions is precisely the change in total mass above. The sum of the right-hand sides is zero. Hence, the equations together with the interface conditions preserve total mass.

Remark 3. *The transition conditions as defined above allow organisms to get trapped in a given patch or set of patches. For example, consider* $[0, L_1]$ *as a patch of type 1 and* $[L_1, L_1 + L_2]$ *as an adjacent patch of type 2 (see Figure 1). The probability of not leaving patch 1 at* $x = 0$ *is* $1-\beta^-$ *and the probability of not leaving patch 2 at* $x = L$ *is* $1-\beta^+$*. Hence, the probability of getting stuck in these two patches is* $P_{trap} = (1-\beta^+)(1-\beta^-)$*. For small values of* $\beta^\pm$*, this probability is significant. We will see its importance when we study the speed of travelling wave solutions. For convenience, we also define the probability of moving on, which is* $1 - P_{trap} = 1-(1-\beta^+)(1-\beta^-) = \beta^+\beta^- - \beta^+ - \beta^-$.

We observe that the interface conditions contain not only the movement preference at the interface ($\beta^\pm$) but also the movement behaviour in the adjacent patches ($\gamma_i\mu_i$). This is analogous to the parabolic case [30, 36]. In the next section, we derive the parabolic limit of the correlated random walk in a patchy landscape.

3.1. The parabolic limit of the patchy system with interface

We take the parabolic limit of system (3.1) in each patch similar to (1.6) with

$$D_i=\lim_{\lambda_i,\gamma_i\to\infty}\frac{\gamma_i^2\mu_i}{2\lambda_i} \tag{3.9}$$

and arrive at

$$u_t = D_iu_{xx}, \tag{3.10}$$

where $u = u^+ + u^-$. We need to find conditions at the interface $x = 0$ that relate $u(0^\pm, t)$ and $u_x(0^\pm, t)$. We use the relations as before

$$2u^+ = u+\frac{1}{\gamma_i}v, \qquad 2u^- = u-\frac{1}{\gamma_i}v. \tag{3.11}$$

Substituting these two expressions into (3.6), we find

$$u(0^+,t)+\frac{1}{\gamma_1}v(0^+,t) = \beta^+\frac{\mu_2\gamma_2}{\mu_1\gamma_1}\left(u(0^-,t)+\frac{1}{\gamma_2}v(0^-,t)\right) \tag{3.12}$$

$$+(1-\beta^-)\left(u(0^+,t)-\frac{1}{\gamma_1}v(0^+,t)\right). \tag{3.13}$$

In the parabolic limit, we have $\gamma_i \to \infty$ so that the remaining terms are

$$u(0^+,t)=\beta^+\frac{\mu_2\gamma_2}{\mu_1\gamma_1}u(0^-,t)+(1-\beta^-)u(0^+,t). \tag{3.14}$$

This gives us the interface condition

$$u(0^+,t)=\frac{\beta^+}{\beta^-}\frac{\mu_2\gamma_2}{\mu_1\gamma_1}u(0^-,t). \tag{3.15}$$

We note that while γ_i are independent, they need to approach infinity at the same rate in order for the limit to make sense.

As in [30], there are a few special cases. If turning rates and movement probabilities are equal between the two patches and only the step sizes differ, then $\lambda_1 = \lambda_2$, $\mu_1 = \mu_2$ and $\delta_1 \neq \delta_2$, which implies $\gamma_1 \neq \gamma_2$. This leads to the interface condition for the parabolic limits as

$$u(0^+, t) = \frac{\beta^+}{\beta^-}\sqrt{\frac{D_2}{D_1}}u(0^-, t). \tag{3.16}$$

On the other hand, if only the probabilities of moving differ between the patches, i.e., $\mu_1 \neq \mu_2$, but $\gamma_1 = \gamma_2$, we find

$$u(0^+, t) = \frac{\beta^+}{\beta^-}\frac{D_2}{D_1}u(0^-, t). \tag{3.17}$$

Both of these cases have been derived and discussed previously in the parabolic setting in [30]. Finally, if only the turning rates differ, then $\lambda_1 \neq \lambda_2$, but $\mu_1 = \mu_2$ and $\gamma_1 = \gamma_2$, we find

$$u(0^+, t) = \frac{\beta^+}{\beta^-}u(0^-, t). \tag{3.18}$$

We showed earlier that the hyperbolic system preserves total mass, and the same is true in the limiting parabolic system. Hence, we get the expected flux-matching conditions for the parabolic limit as

$$D_1 u_x(0^+, t) = D_2 u_x(0^-, t). \tag{3.19}$$

3.2. Homogenization in patchy landscapes

In this section, we consider the patchy CRW (3.1) in a periodic landscape of two alternating patch types. We denote the length of patches of type i as L_i (see Figure 1). At each interface, we have matching conditions of the form in (3.6), (3.7) or (3.8), depending on whether patch type 1 is to the right or the left of the interface. Under the assumption that the period is small, we derive the homogenization limit of the equations. To keep track of the various parameters and their meaning, we summarize the most important relations in Table 1.

We will use some convenient combinations of parameters. As μ_i denotes the motility (probability to move), and γ_i is the particle speed when it moves, the product $\mu_i\gamma_i$ denotes the net speed of particles in patch $i = 1, 2$. If we multiply the net speed $\gamma_1\mu_1$ by the transition probability β_0^-, we get the net transition speed of particles moving from patch 1 into patch 2. This leads us to define two ratios of the speeds involved:

$$k = \frac{\mu_2\gamma_2}{\mu_1\gamma_1}, \qquad \kappa = \frac{\beta^+ k}{\beta^-} = \frac{\beta^+\mu_2\gamma_2}{\beta^-\mu_1\gamma_1}. \tag{3.20}$$

The coefficient k is the ratio of the net moving speeds of patch 2 over patch 1, and κ denotes the ratio of the transition speed from patch 1 to patch 2 over the net transition speed from patch 2 to patch 1.

Theorem 2. *The homogenization of (3.1) with jump boundary conditions (3.6,3.7,3.8), and coefficients that are L-periodic in y, $L = L_1 + L_2$, is given by*

$$\begin{aligned} f_t^+ + \tilde{\gamma} f_x^+ &= \tilde{\lambda}(f^- - f^+), \\ f_t^- - \tilde{\gamma} f_x^- &= \tilde{\lambda}(f^+ - f^-), \end{aligned} \tag{3.21}$$

Table 1. Table of parameters and symbols related to the patchy landscape.

Expression	Meaning
γ_i	speed in patch $i \in \{1, 2\}$
μ_i	probability that a particle in patch i moves
λ_i	turning rate in patch i
$\mu_i\gamma_i$	effective speed in patch i
$k = \frac{\mu_2\gamma_2}{\mu_1\gamma_1}$	ratio of net particle speeds in patch 2 versus 1.
$D_i = \frac{\gamma_i^2\mu_i}{2\lambda_i}$	effective diffusion constant in patch i
$\beta^{\pm}$	probability that and individual that arrived at an interface moving to the right (left) continues right (left)
$1-\beta^{\pm}$	probability of turning at the patch interface
$\beta^-\mu_1\gamma_1$	net transition speed from patch 1 to patch 2
$\beta^+\mu_2\gamma_2$	net transition speed from patch 2 to patch 1
$\kappa = \frac{\beta^+}{\beta^-}k = \frac{\beta^+\mu_2\gamma_2}{\beta^-\mu_1\gamma_1}$	ratio of net transition speeds over the patch boundaries.
$h(y) = \begin{cases} 1 & y \in \text{ patch 1} \\ \kappa & y \in \text{ patch 2} \end{cases}$	local scaling function
$u_0^{\pm}(x, y, t) = \frac{f^{\pm}(x,t)}{h(y)}$	leading order term

with

$$u_0^{\pm}(x, y, t) = \frac{f^{\pm}(x, t)}{h(y)}, \qquad h(y) = \begin{cases} 1, & y \in (y_0, y_1), \\ \kappa, & y \in (y_1, y_2). \end{cases} \tag{3.22}$$

Here

$$\tilde{\gamma} = \langle\gamma\mu\rangle_{wh} = \frac{\left\langle \frac{1}{h} \right\rangle_a}{\left\langle \frac{1}{\gamma\mu h} \right\rangle_a} = \frac{L_1 + \frac{L_2}{\kappa}}{\frac{L_1}{\gamma_1\mu_1} + \frac{L_2}{\gamma_2\mu_2\kappa}} \tag{3.23}$$

is the weighted harmonic mean of $\gamma\mu$ with weights L_1 and $\frac{L_2}{\kappa}$, and

$$\tilde{\lambda} = \frac{\left\langle \frac{\lambda}{\gamma h} \right\rangle_a}{\left\langle \frac{1}{\gamma\mu h} \right\rangle_a} = \langle\gamma\mu\rangle_{wh} \left\langle \frac{\lambda}{\gamma} \right\rangle_{wa}, \tag{3.24}$$

where $\langle\cdot\rangle_{wa}$ denotes the weighted arithmetic mean with the same weights.

Proof. We denote the interface locations by y_i with $i = 0, \pm1, \pm2, \ldots$. We have $y_1 - y_0 = L_1$ and $y_2 - y_1 = L_2$ as the length of patches of type 1 and 2, respectively (see Figure 1). The landscape repeats periodically from thereon. We treat the period $L = L_1 + L_2 = \epsilon$ as a small parameter.

We write the density functions $u^{\pm}(x, y, t)$ as functions of the large and small scale variables, x and $y = x/\epsilon$, and we denote the parameter functions $\gamma = \gamma(y)$ as γ_i on patch type $i = 1, 2$, and similarly for λ_i and μ_i. Considering x and y as independent variables gives us the equations

$$\begin{aligned} u_t^+ + (\gamma\mu(u_x^+ + \epsilon^{-1}u_y^+)) &= \mu\lambda(u^- - u^+), \\ u_t^- - (\gamma\mu(u_x^- + \epsilon^{-1}u_y^-)) &= \mu\lambda(u^+ - u^-). \end{aligned} \tag{3.25}$$

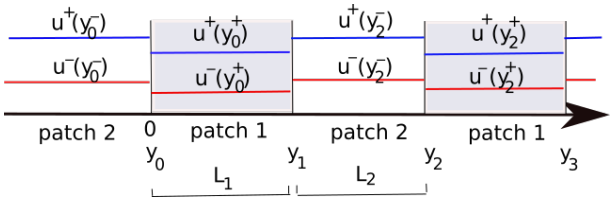

Figure 2. Balancing the boundary transitions for a piecewise constant solution.

The interface conditions (3.6) and (3.7) can be written in matrix form. For example, at y_0 we have

$$\begin{bmatrix} u^+(\cdot, y_0^+, \cdot) \\ u^-(\cdot, y_0^-, \cdot) \end{bmatrix} = \begin{bmatrix} \beta^+ k & (1-\beta^-) \\ (1-\beta^+) & \beta^-/k \end{bmatrix} \begin{bmatrix} u^+(\cdot, y_0^-, \cdot) \\ u^-(\cdot, y_0^+, \cdot) \end{bmatrix} =: A_0 \begin{bmatrix} u^+(\cdot, y_0^-, \cdot) \\ u^-(\cdot, y_0^+, \cdot) \end{bmatrix},$$

where we use k from (3.20). Similarly, at y_1, we have

$$\begin{bmatrix} u^+(\cdot, y_1^+, \cdot) \\ u^-(\cdot, y_1^-, \cdot) \end{bmatrix} = \begin{bmatrix} \beta^-/k & (1-\beta^+) \\ (1-\beta^-) & \beta^+ k \end{bmatrix} \begin{bmatrix} u^+(\cdot, y_1^-, \cdot) \\ u^-(\cdot, y_1^+, \cdot) \end{bmatrix} =: A_1 \begin{bmatrix} u^+(\cdot, y_1^-, \cdot) \\ u^-(\cdot, y_1^+, \cdot) \end{bmatrix}.$$

We expand the densities as

$$u^\pm(x, y, t) = \sum_n \epsilon^n u_n^\pm(x, y, t), \tag{3.26}$$

where $u_n^\pm$ are L-periodic with respect to y. The interface conditions contain only densities and no derivatives. Therefore, they hold for each term in the series expansion.

We substitute (3.26) into (3.25) and consider orders of ε. The equations of order ϵ^{-1} are simply

$$u_{0,y}^\pm = 0$$

in each patch. Hence, the functions $u_0^\pm$ are constant with respect to y in each patch (see Figure 2). We calculate the size of the jumps across the interfaces. To simplify notation, we write $u_0^\pm(\cdot, y, \cdot) = U^\pm(y)$. Then we use the fact that $U^\pm$ are constant on each patch, L-periodic, and satisfy the interface conditions as illustrated in Figure 2. We calculate

$$\begin{aligned} \begin{bmatrix} U^+(y_0^+) \\ U^-(y_0^-) \end{bmatrix} &= A_0 \begin{bmatrix} U^+(y_0^-) \\ U^-(y_0^+) \end{bmatrix} = A_0 \begin{bmatrix} U^+(y_2^-) \\ U^-(y_0^+) \end{bmatrix} = A_0 \begin{bmatrix} U^+(y_1^+) \\ U^-(y_1^-) \end{bmatrix} \\ &= A_0 A_1 \begin{bmatrix} U^+(y_1^-) \\ U^-(y_1^+) \end{bmatrix} = A_0 A_1 \begin{bmatrix} U^+(y_0^+) \\ U^-(y_2^-) \end{bmatrix} = A_0 A_1 \begin{bmatrix} U^+(y_0^+) \\ U^-(y_0^-) \end{bmatrix}. \end{aligned}$$

In particular, the vector $[U^+(y_0^+), U^-(y_0^-)]^T$ is an eigenvector of the matrix $A_0 A_1$ with eigenvalue 1. We check that the matrix has indeed such an eigenvalue and we calculate the eigenvector. We find

$$A_0 A_1 = \begin{bmatrix} \beta^+\beta^- + (1-\beta^-)^2 & \beta^+ k(2-\beta^+-\beta^-) \\ \frac{\beta^-(2-\beta^+-\beta^-)}{k} & \beta^+\beta^- + (1-\beta^+)^2 \end{bmatrix}.$$

It is straight forward to calculate $\det(I - A_0 A_1) = 0$, to see that this matrix does indeed have an eigenvalue equal to unity. Furthermore, we calculate the right eigenvector as

$$\begin{bmatrix} U^+(y_0^+) \\ U^-(y_0^-) \end{bmatrix} = r \begin{bmatrix} \beta^+ k \\ \beta^- \end{bmatrix}, \quad \text{and} \quad \begin{bmatrix} U^+(y_1^+) \\ U^-(y_1^-) \end{bmatrix} = r A_1 \begin{bmatrix} \beta^+ k \\ \beta^- \end{bmatrix} = r \begin{bmatrix} \beta^- \\ \beta^+ k \end{bmatrix}, \tag{3.27}$$

for $r \in \mathbb{R}$. Hence, the ratio of the densities across the interface(s) is the same for U^+ and U^-, and it is given by $U^+(y_1^+)/U^+(y_0^+) = U^-(y_0^-)/U^-(y_1^-) = \frac{\beta_0^-}{\beta_0^+ k} = \frac{1}{\kappa}$, with κ from (3.20). Using $h(y)$ from (3.22) we can write the densities as

$$u_0^\pm(x, y, t) = \frac{f^\pm(x, t)}{h(y)}, \tag{3.28}$$

where $f^\pm$ are independent of y.

Next, we consider the equations of order ϵ^0. They are

$$\begin{aligned} u_{0,t}^+ + (\gamma\mu(u_{0,x}^+ + u_{1,y}^+)) &= \mu\lambda(u_0^- - u_0^+), & (3.29)\\ u_{0,t}^- - (\gamma\mu(u_{0,x}^- + u_{1,y}^-)) &= \mu\lambda(u_0^+ - u_0^-). & (3.30) \end{aligned}$$

We solve for $u_{1,y}^\pm$ and find

$$\begin{aligned} u_{1,y}^+ &= \frac{1}{\gamma\mu h}\left[\lambda\mu(f^- - f^+) - f_t^+ - \gamma\mu f_x^+\right], & (3.31)\\ u_{1,y}^- &= \frac{1}{\gamma\mu h}\left[-\lambda\mu(f^+ - f^-) + f_t^- - \gamma\mu f_x^-\right]. & (3.32) \end{aligned}$$

We integrate the left-hand side over n periods and calculate

$$\begin{aligned} \int_{y_0}^{y_{2n}} u_{1,y}^+ dy &= \sum_{j=0}^{2n} (u_1^+(y_j^-) - u_1^+(y_{j-1}^+)) \\ &= u_1^+(y_{2n}^-) - \sum_{j=1}^{2n-1} (u_1^+(y_j^+) - u_1^+(y_{j-1}^-)) - u_1^+(y_0^+) \\ &= n\left([u_1^+(y_0)] + [u_1^+(y_1)]\right), \end{aligned}$$

where we used periodicity so that $u_1^+(y_{2n}^-) = u_1^+(y_0^-)$ and the standard jump notation

$$[u(y)] = u(y^+) - u(y^-).$$

A similar expression holds for u_1^-.

If $u_1^\pm$ are to remain bounded as y (or n) become large, we necessarily have

$$[u_1^\pm(y_0)] + [u_1^\pm(y_1)] = 0.$$

Hence, the integral on the right hand side of (3.31) and (3.32) must equal zero as well. The functions $f^\pm$ are independent of the small-scale variable y; only the parameter functions γ, μ, λ and the scaling function h depend on y and are L-periodic in y. Integrating (3.31) over one period gives the condition

$$0 = \left\langle \frac{\lambda}{\gamma h} \right\rangle_a (f^- - f^+) - \left\langle \frac{1}{\gamma\mu h} \right\rangle_a f_t^+ - \left\langle \frac{1}{h} \right\rangle_a f_x^+. \tag{3.33}$$

where the arithmetic means are given by

$$\left\langle \frac{\lambda}{\gamma h} \right\rangle_a = \frac{1}{L_1 + L_2}\left(\frac{L_1\lambda_1}{\gamma_1} + \frac{L_2\lambda_2}{\gamma_2\kappa}\right), \tag{3.34}$$

and similarly for the other terms. The corresponding condition for f^- can be derived from (3.32). Dividing by the coefficient of $f_t^\pm$, we find the homogenized equations (3.21). □

4. Reaction random walk systems

In this section, we include birth and death dynamics into the patchy CRW, as done previously in the spatially homogeneous case (1.9). The equations are

$$\begin{aligned} u_t^+ + \gamma(x)(\mu(x)u)_x^+ &= \mu(x)\lambda(x)(u^- - u^+) + G^+(u^+, u^-, x), \\ u_t^- - \gamma(x)(\mu(x)u)_x^- &= \mu(x)\lambda(x)(u^+ - u^-) + G^-(u^+, u^-, x), \end{aligned} \tag{4.1}$$

where, for the sake of convenience, we wrote the parameters as piecewise constant functions, i.e., $\mu(x) = \mu_i$ in patches of type i, and similarly for the other parameters. The form of the growth and death terms $G^\pm$ was given in (1.10); we will use the same subscript notation for $G_i^\pm$ below.

4.1. Homogenization including reactions

We assume that the reaction terms also vary only on the small scale, i.e., we write $G^\pm(u^+, u^-, y)$ in (4.1), and we assume that $G^\pm$ are L-periodic in y.

Theorem 3. *The homogenization of (4.1) with L-periodic coefficients is given by*

$$\begin{aligned} f_t^+ + \tilde{\gamma} f_x^+ &= \tilde{\lambda}(f^- - f^+) + \tilde{G}^+(f^+, f^-), \\ f_t^- - \tilde{\gamma} f_x^- &= \tilde{\lambda}(f^+ - f^-) + \tilde{G}^-(f^+, f^-), \end{aligned} \tag{4.2}$$

where $f^\pm$ is given by (3.28), $\tilde{\gamma}$ and $\tilde{\lambda}$ are as above in (3.23) and (3.24), and

$$\tilde{G}^\pm = \frac{\frac{L_1}{\mu_1\gamma_1} G_1^\pm(f^+, f^-) + \frac{L_2}{\mu_2\gamma_2\kappa}\kappa G_2^\pm\left(\frac{f^+}{\kappa}, \frac{f^-}{\kappa}\right)}{\frac{L_1}{\mu_1\gamma_1} + \frac{L_2}{\mu_2\gamma_2\kappa}}. \tag{4.3}$$

Note that $\tilde{G}^+$ from (1.10) is a weighted arithmetic mean of hG^+ with weights $\frac{L_i}{\gamma_i\mu_i h_i}$. If we use the explicit form of $G_i^\pm = \frac{m_i(u)}{2}u - g_i(u)u^\pm$, then we obtain the homogenization as

$$\begin{aligned} f_t^+ + \tilde{\gamma} f_x^+ &= \tilde{\lambda}(f^- - f^+) + \tfrac{\tilde{m}(f)}{2}(f^+ + f^-) - \tilde{g}(f)f^+, \\ f_t^- - \tilde{\gamma} f_x^- &= \tilde{\lambda}(f^+ - f^-) + \tfrac{\tilde{m}(f)}{2}(f^+ + f^-) - \tilde{g}(f)f^-, \end{aligned} \tag{4.4}$$

with $f = f^+ + f^-$ and

$$\tilde{m}(f) = \frac{\frac{L_1}{\mu_1\gamma_1} m_1(f) + \frac{L_2}{\mu_2\gamma_2\kappa} m_2(f/\kappa)}{\frac{L_1}{\mu_1\gamma_1} + \frac{L_2}{\mu_2\gamma_2\kappa}}, \qquad \tilde{g}(f) = \frac{\frac{L_1}{\mu_1\gamma_1} g_1(f) + \frac{L_2}{\mu_2\gamma_2\kappa} g_2(f/\kappa)}{\frac{L_1}{\mu_1\gamma_1} + \frac{L_2}{\mu_2\gamma_2\kappa}}. \tag{4.5}$$

Proof. To start the analysis, we write the equations as a two-scale problem, using (2.4) as

$$\begin{aligned} u_t^+ + (\gamma\mu(u_x^+ + \epsilon^{-1}u_y^+)) &= \mu\lambda(u^- - u^+) + G^+(u^+, u^-, y), \\ u_t^- - (\gamma\mu(u_x^- + \epsilon^{-1}u_y^-)) &= \mu\lambda(u^+ - u^-) + G^-(u^+, u^-, y). \end{aligned}$$

To homogenize, we follow the same steps as in Section 3.2. The equations of order ϵ^{-1} are unchanged. Hence, we arrive at the same result as in (3.28), namely $u_0^\pm(x, y, t) = \frac{f^\pm(x,t)}{h(y)}$, where $f^\pm$ are independent of y, and $h(y)$ is given by (3.28).

The equations of order ϵ^0 are now given by

$$\begin{aligned} u^+_{0,t} + (\gamma\mu(u^+_{0,x} + u^+_{1,y})) &= \mu\lambda(u^-_0 - u^+_0) + G^+(u^+_0, u^-_0, y), \\ u^-_{0,t} - (\gamma\mu(u^-_{0,x} + u^-_{1,y})) &= \mu\lambda(u^+_0 - u^-_0) + G^-(u^+_0, u^-_0, y). \end{aligned}$$

Just as before, we solve for $u^\pm_{1,y}$ and find

$$u^+_{1,y} = \frac{1}{\gamma\mu h}\left[\lambda\mu(f^- - f^+) + hG^+\left(\frac{f^+}{h}, \frac{f^-}{h}, y\right) - f^+_t - \gamma\mu f^+_x\right],$$

and similarly for $u^-_{1,y}$.

The next steps proceed as above. Integrating over n periods on the left-hand side produces zero. Hence, integrating over the right-hand side must do the same. Then we have the analogue of (3.33), which is

$$0 = \left\langle\frac{\lambda}{\gamma h}\right\rangle_a (f^- - f^+) + \left\langle\frac{G^+}{\gamma\mu}\right\rangle_a - \left\langle\frac{1}{\gamma\mu h}\right\rangle_a f^+_t - \left\langle\frac{1}{h}\right\rangle_a f^+_x.$$

Solving for f^+_t (and doing all the steps for the equation for f^-_t) gives the homogenized system

$$\begin{aligned} f^+_t + \tilde{\gamma} f^+_x &= \tilde{\lambda}(f^- - f^+) + \tilde{G}^+(f^+, f^-), \\ f^-_t - \tilde{\gamma} f^-_x &= \tilde{\lambda}(f^+ - f^-) + \tilde{G}^-(f^+, f^-), \end{aligned}$$

where $\tilde{\gamma}$, and $\tilde{\lambda}$ are as above and $\tilde{G}^\pm$ as in (4.3). □

5. Species persistence and invasion

To apply our results to a real-world problem, we choose to study the following questions regarding the persistence and spread of a population in a heterogeneous landscape:

1. What portion of a periodic landscape needs to consist of "good" patches such that the population can persist globally?
2. Suppose that the population can persist globally, how fast will it spread globally when introduced into a good patch?

For our analysis, we make the standard assumption that the population does not experience an Allee effect. An Allee effect occurs when the maximum per capita growth rate is not at low but intermediate population densities. If there is no Allee effect, then questions of persistence and extinction as well as the calculation of the spread rate can typically be answered by studying the linearization of the model at the trivial state. We will use this assumption. We use two methods to answer these questions: the homogenization derived earlier and exact analytical expressions for the full periodic system.

The linearization of $G^\pm_i = \frac{m_i(u)}{2}u - g_i(u)u^\pm$ at the trivial steady state is given by $\frac{m_i(0)}{2}u - g_i(0)u^\pm$. For simplicity, we drop the argument and write simply m_i and g_i for the birth and death rate parameters at low density. If the growth rate exceeds the death rate in a given patch type, i.e., $m_i > g_i$, we speak of a "good" patch; if the inequality is reversed, we speak of a "bad" patch. If both patch types in the landscape are good then the population can persist in each type and hence also in the heterogeneous landscape. We consider the more interesting case that only type-1-patches are good ($m_1 > g_1$) and allow for local persistence. Type-2-patches are bad ($m_2 < g_2$) and would lead to local extinction in the absence of movement (see Figure 3).

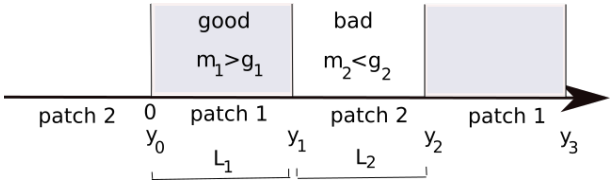

Figure 3. Habitats of varying quality.

5.1. Calculation of the persistence conditions

First, we ask for the minimum fraction of type-1 patches that allows for global persistence. We define persistence to mean that the zero steady state is unstable. We begin with the homogenization approach and we linearize the homogenized equation (4.2) at zero:

$$\begin{aligned} f_t^+ + \tilde{\gamma} f_x^+ &= \tilde{\lambda}(f^- - f^+) + \tfrac{\tilde{m}}{2}(f^+ + f^-) - \tilde{g} f^+, \\ f_t^- - \tilde{\gamma} f_x^- &= \tilde{\lambda}(f^+ - f^-) + \tfrac{\tilde{m}}{2}(f^+ + f^-) - \tilde{g} f^-. \end{aligned} \tag{5.1}$$

where

$$\tilde{m} = \frac{\frac{L_1}{\mu_1\gamma_1} m_1 + \frac{L_2}{\mu_2\gamma_2\kappa} m_2}{\frac{L_1}{\mu_1\gamma_1} + \frac{L_2}{\mu_2\gamma_2\kappa}}, \qquad \tilde{g} = \frac{\frac{L_1}{\mu_1\gamma_1} g_1 + \frac{L_2}{\mu_2\gamma_2\kappa} g_2}{\frac{L_1}{\mu_1\gamma_1} + \frac{L_2}{\mu_2\gamma_2\kappa}}$$

using the abbreviation

$$m_i = m_i(0), \qquad g_i = g_i(0), \qquad i = 1, 2.$$

Since we work on the entire real line and since the equation is homogeneous, we can consider spatially homogeneous solutions. Then the flux is zero and the total density $f = f^+ + f^-$ satisfies

$$f_t = (\tilde{m} - \tilde{g}) f.$$

Hence our homogenized persistence condition becomes

$$\begin{aligned} \tilde{m} &> \tilde{g} \\ \frac{L_1}{\mu_1\gamma_1} m_1 + \frac{L_2}{\mu_2\gamma_2\kappa} m_2 &> \frac{L_1}{\mu_1\gamma_1} g_1 + \frac{L_2}{\mu_2\gamma_2\kappa} g_2 \\ \frac{L_1}{\mu_1\gamma_1}(m_1 - g_1) &> \frac{L - L_1}{\mu_2\gamma_2\kappa}(g_2 - m_2) \qquad (5.2) \\ \frac{L_1}{L} &> \frac{\mu_1\gamma_1(g_2 - m_2)}{\mu_1\gamma_1(g_2 - m_2) + \mu_2\gamma_2\kappa(m_1 - g_1)} \qquad (5.3) \end{aligned}$$

Inequality (5.2) allows an insightful biological interpretation. Since L_1 has units of length and $\mu_1\gamma_1$ units of velocity, the ratio $\frac{L_1}{\mu_1\gamma_1}$ is a time. It is the time that an individual needs to traverse a patch of length L_1. This is multiplied by the effective growth rate $m_1 - g_1$. Hence the left-hand side $\frac{L_1}{\mu_1\gamma_1}(m_1 - g_1)$ denotes the population growth or decay while a particle is traversing patch 1. Similarly, $\frac{L_2}{\mu_2\gamma_2}(m_2 - g_2)$ denotes the net growth during the time that a particle needs to traverse a patch of type 2. This factor is multiplied by the scaling factor κ, which arises from the jump-boundary conditions. Then (5.2) balances the net growth while in patch 1 with the net growth in patch 2, scaled by the interface factor κ.

We illustrate the persistence condition (5.3) by plotting the relation where the inequality becomes an equality. We fix all values except m_2 and L_1. Then the ratio L_1/L becomes a function of m_2, which we plot as a dashed black line in Figure 4.

To compare this result with the full periodic system (4.1), we linearize (4.1) at zero and get

$$\begin{aligned} u_t^+ + \gamma_i\mu_i u_x^+ &= \mu_i\lambda_i(u^- - u^+) + \tfrac{m_i}{2}(u^+ + u^-) - g_i u^+, \\ u_t^- - \gamma_i\mu_i u_x^- &= \mu_i\lambda_i(u^+ - u^-) + \tfrac{m_i}{2}(u^+ + u^-) - g_i u^-, \end{aligned} \tag{5.4}$$

on patches $i = 1, 2$ of length $L_{1,2}$, with $m_i = m_i(0), g_i = g_i(0)$ as above. We have the linear interface conditions from (3.6), i.e.

$$u^+(0^+, t) = \beta^+ k u^+(0^-, t) + (1-\beta^-)u^-(0^+, t), \tag{5.5}$$

$$u^-(0^-, t) = (1-\beta^+)u^+(0^-, t) + \frac{\beta^-}{k}u^-(0^+, t), \tag{5.6}$$

with k from (3.20).

We make the ansatz

$$u^\pm(x, t) = e^{\nu t}\phi^\pm(x),$$

where $\phi^\pm$ are $L_1 + L_2 = L$-periodic functions. Then the population can grow if $\nu > 0$ and will decline if $\nu < 0$. The persistence boundary is given by $\nu = 0$.

Substituting the ansatz into the above Eqs (5.4), we obtain the system

$$\frac{d}{dx}\begin{bmatrix}\phi^+ \\ \phi^-\end{bmatrix} = M_i \begin{bmatrix}\phi^+ \\ \phi^-\end{bmatrix},$$

where matrices M_i are given by

$$M_i = \frac{1}{\gamma_i\mu_i}\begin{bmatrix} A_i - \nu & B_i \\ -B_i & -(A_i - \nu)\end{bmatrix} \quad \text{with} \quad \begin{cases} A_i = \frac{m_i}{2} - g_i - \mu_i\lambda_i, \\ B_i = \frac{m_i}{2} + \mu_i\lambda_i. \end{cases}$$

We solve the interface conditions as follows (we suppress the t-dependence for notational convenience):

$$\begin{aligned} u^-(0^+) &= \frac{k}{\beta^-}\Big((\beta^+ - 1)u^+(0^-) + u^-(0^-)\Big) \\ u^+(0^+) &= \left(\beta^+ k + \frac{k(1-\beta^-)(\beta^+ - 1)}{\beta^-}\right)u^+(0^-) + \frac{k(1-\beta^-)}{\beta^-}u^-(0^-). \end{aligned} \tag{5.7}$$

These conditions can be written in matrix form as

$$\begin{bmatrix}u^+(0^+) \\ u^-(0^+)\end{bmatrix} = S_0 \begin{bmatrix}u^+(0^-) \\ u^-(0^-)\end{bmatrix}$$

and similarly at $x = L_1$ with some matrix S_1. The explicit expressions are

$$S_0 = \begin{bmatrix}\beta^+ k + \frac{k(1-\beta^-)(\beta^+-1)}{\beta^-} & \frac{k(1-\beta^-)}{\beta^-} \\ \frac{k(\beta^+-1)}{\beta^-} & \frac{k}{\beta^-}\end{bmatrix} \tag{5.8}$$

and

$$S_1 = \begin{bmatrix} \frac{\beta^-}{k} + \frac{(1-\beta^+)(\beta^- - 1)}{\beta^+ k} & \frac{1-\beta^+}{\beta^+ k} \\ \frac{\beta^- - 1}{\beta^+ k} & \frac{1}{\beta^+ k} \end{bmatrix}. \tag{5.9}$$

With these expressions, we can solve the linear equations for $\phi^{\pm}$. We have

$$\begin{bmatrix} \phi^+ \\ \phi^- \end{bmatrix}(L^+) = S_0 \begin{bmatrix} \phi^+ \\ \phi^- \end{bmatrix}(L^-) = S_0 e^{M_2(L-L_1)} \begin{bmatrix} \phi^+ \\ \phi^- \end{bmatrix}(L_1^+) \tag{5.10}$$

$$= S_0 e^{M_2(L-L_1)} S_1 \begin{bmatrix} \phi^+ \\ \phi^- \end{bmatrix}(L_1^-) = S_0 e^{M_2(L-L_1)} S_1 e^{M_1(L_1)} \begin{bmatrix} \phi^+ \\ \phi^- \end{bmatrix}(0^+). \tag{5.11}$$

Periodicity requires $\phi^{\pm}(L^+) = \phi^{\pm}(0^+)$, so that we obtain the eigenvalue problem

$$\begin{bmatrix} \phi^+ \\ \phi^- \end{bmatrix}(0^+) = S_0 e^{M_2(L-L_1)} S_1 e^{M_1 L_1} \begin{bmatrix} \phi^+ \\ \phi^- \end{bmatrix}(0^+) \tag{5.12}$$

Hence, we have proved the following result.

Lemma 3. *The persistence boundary $\nu = 0$ is given by the condition that the matrix in (5.12) have a dominant eigenvalue equal to unity.*

To find the threshold between persistence and extinction, we set $\nu = 0$ and solve the resulting eigenvalue problem numerically. We fix parameters except m_2 and L_1. Then we calculate $\frac{L_1}{L}$ as a function of m_2. Since we fix the period $L = L_1 + L_2$, we interpret L_1/L as a fraction of good habitat patches required for persistence. As expected, the minimum fraction of required good habitat decreases as the birth rate m_2 of the bad habitat increases, see Figure 4.

The homogeneous persistence condition approximates the exact condition as L becomes small (top left plot). The top right plot in Figure 4 illustrates that the approximation is better when the speeds and turning rates are high, i.e., when we are closer to the parabolic limit. The bottom plot shows that the homogenization is better when individuals have a high probability of continuing movement across patch boundaries ($\beta^{\pm} \approx 1$). When individuals frequently turn at a patch boundary, they might get stuck within a patch or set of patches; see Remark 3. If they do, then the loss of individuals due to mortality in bad patches is decreased, so that the population can persist on less good habitat.

5.2. Invasion speeds

To calculate invasion speeds, we rely on the linear conjecture that under certain conditions the spreading speed of the nonlinear model is given by the spreading speed of the linear model, which, in turn, is the minimal traveling wave speed of the linear model. The linearized homogenized model (4.2) is of the form of a general reaction CRW system (1.9), as discussed in Section 1.2. According to (1.14), the minimal wave speed of this equation is

$$c^* = \frac{2\tilde{\gamma}}{\tilde{m} + 2\tilde{\lambda}} \sqrt{(\tilde{m} - \tilde{g})(2\tilde{\lambda} + \tilde{g})}\,. \tag{5.13}$$

To calculate the dispersion relation of the linearized patchy reaction CRW system, we adapt the techniques that Shigesada and others [40] developed for the parabolic case to the hyperbolic case. We choose $G^{\pm}$ as above. We linearize the model at low density and obtain the equations

$$u_t^+ + \gamma_i \mu_i u_x^+ \;=\; \mu_i \lambda_i (u^- - u^+) + m_i (u^+ + u^-)/2 - g_i u^+, \tag{5.14}$$

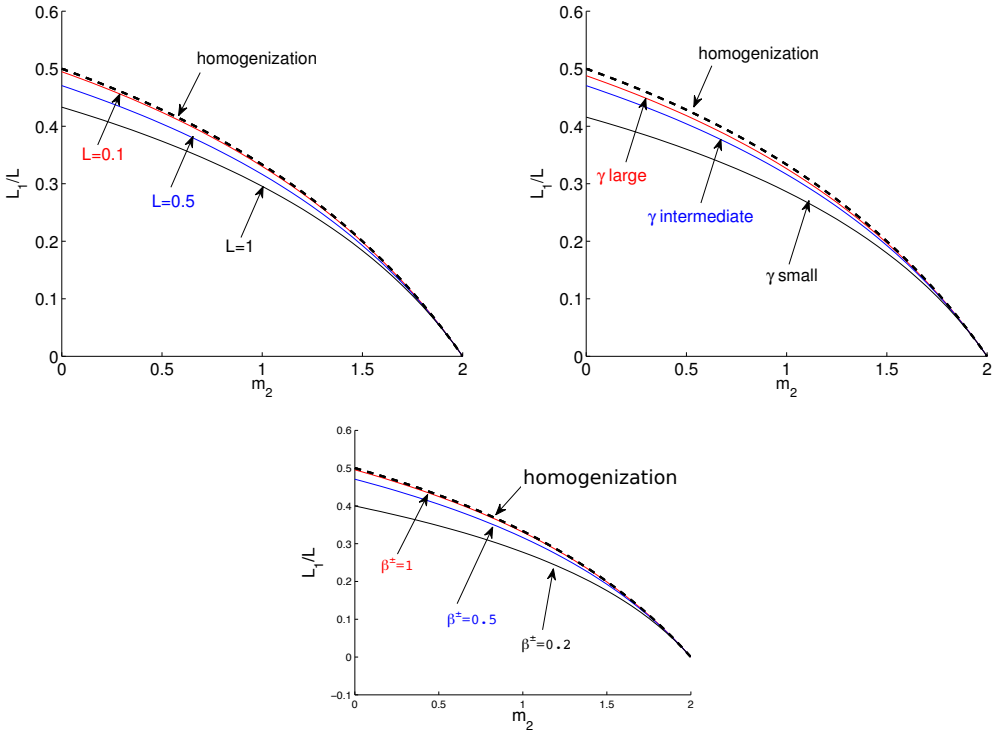

Figure 4. Percentage of good habitat required for population persistence according to the homogenized model (black dashes) and the exact condition in Lemma 3. **Top left plot:** As L decreases, the fit gets better, as expected. Parameter values are $L = 1$ (black), $L = 0.5$ (blue) and $L = 0.1$ (red), as well as $\gamma_i = 5$ and $\lambda_i = 10$. **Top right plot:** as γ_i and λ_i increase, while keeping the ratio $\gamma^2/(2\lambda)$ constant, the fit gets better. Parameter values are $\lambda_i = 100$ (red), $\lambda_i = 10$, (blue) and $\lambda_1 = 1$ (black), as well as $L = 0.5$. **Bottom plot:** The fit is better for $\beta^{\pm} \approx 1$ and gets worse as $\beta^{\pm}$ decrease. Parameter values are $\beta^{\pm} = 0.9$ (red), $\beta^{\pm} = 0.5$ (blue), and $\beta^{\pm} = 0.2$ (black) as well as $\gamma_i = 5$ and $\lambda_i = 10$ and $L = 0.5$. (The blue curves are identical in the three plots.) The two patch types differ only in the growth and death rates. Common parameters are $\mu_i = 1, \beta^{\pm} = 0.5, m_1 = 3 > 1 = m_2$, and $g_1 = 1 < 2 = g_2$.

$$u_t^- - \gamma_i \mu_i u_x^- = \mu_i \lambda_i (u^+ - u^-) + m_i (u^+ + u^-)/2 - g_i u^-, \tag{5.15}$$

on patches $i = 1, 2$ of length L_i. We have the interface conditions from (3.6), i.e.,

$$u^+(0^+, t) = \beta^+ k u^+(0^-, t) + (1 - \beta^-) u^-(0^+, t), \tag{5.16}$$

$$u^-(0^-, t) = (1 - \beta^+) u^+(0^-, t) + (\beta^-/k) u^-(0^+, t), \tag{5.17}$$

with $k = \frac{\mu_2 \gamma_2}{\mu_1 \gamma_1}$.

We make the ansatz of a traveling periodic wave as

$$u^{\pm}(x, t) = e^{-s(x-ct)} \phi^{\pm}(x),$$

where $\phi^{\pm}$ are $L_1 + L_2$-periodic functions. Here, c denotes the speed of the wave and s is steepness at the leading edge. The dispersion relation is the relationship between s and c. We obtain it by substituting

the ansatz into the model equations and deriving conditions, so that nonzero functions ϕ_i exist that satisfy the equations.

We obtain the linear system

$$\frac{d}{dx}\begin{bmatrix}\phi^+\\ \phi^-\end{bmatrix} = N_i \begin{bmatrix}\phi^+\\ \phi^-\end{bmatrix}, \tag{5.18}$$

where matrices N_i are given by

$$N_i = \frac{1}{\gamma_i\mu_i}\begin{bmatrix} A_i - sc + s\gamma_i\mu_i & B_i \\ -B_i & -(A_i - sc - s\gamma_i\mu_i)\end{bmatrix} \quad \text{with} \quad \begin{cases} A_i = m_i/2 - g_i - \mu_i\lambda_i, \\ B_i = m_i/2 + \mu_i\lambda_i. \end{cases} \tag{5.19}$$

We solve the interface conditions as follows:

$$\begin{aligned} u^-(0^+) &= \frac{k}{\beta^-}((\beta^+ - 1)u^+(0^-) + u^-(0^-)), \\ u^+(0^+) &= (\beta^+ k + k(1-\beta^-)(\beta^+ - 1)/\beta^-)u^+(0^-) + k(1-\beta^-)/\beta^- u^-(0^-). \end{aligned} \tag{5.20}$$

These conditions can be written in matrix form as

$$\begin{bmatrix}u^+(0^+)\\ u^-(0^+)\end{bmatrix} = S_0 \begin{bmatrix}u^+(0^-)\\ u^-(0^-)\end{bmatrix},$$

and similarly at $x = L_1$ with some matrix S_1, where S_0 and S_1 are given in (5.8) and (5.9), respectively. We solve system (5.18), starting at $\phi^\pm(0^+)$, and find

$$\begin{bmatrix}\phi^+(L_1^-)\\ \phi^-(L_1^-)\end{bmatrix} = e^{N_1 L_1}\begin{bmatrix}\phi^+(0^+)\\ \phi^-(0^+)\end{bmatrix}.$$

The behaviour at the interface is described by matrix S_1, so that we have

$$\begin{bmatrix}\phi^+(L_1^+)\\ \phi^-(L_1^+)\end{bmatrix} = S_1 e^{N_1 L_1}\begin{bmatrix}\phi^+(0^+)\\ \phi^-(0^+)\end{bmatrix}.$$

Solving the ODE in (5.18) again, this time from L_1 to $L = L_1 + L_2$, we get

$$\begin{bmatrix}\phi^+(L^-)\\ \phi^-(L^-)\end{bmatrix} = e^{N_2 L_2} S_0 e^{N_1 L_1}\begin{bmatrix}\phi^+(0^+)\\ \phi^-(0^+)\end{bmatrix},$$

and finally, by applying the interface conditions at $x = 0$ and periodicity,

$$\begin{bmatrix}\phi^+(0^+)\\ \phi^-(0^+)\end{bmatrix} = \begin{bmatrix}\phi^+(L^+)\\ \phi^-(L^+)\end{bmatrix} = S_0 e^{N_2 L_2} S_1 e^{N_1 L_1}\begin{bmatrix}\phi^+(0^+)\\ \phi^-(0^+)\end{bmatrix}. \tag{5.21}$$

Hence, the initial point of the periodic function is an eigenvector to eigenvalue 1 of this product of four matrices. For a nonzero solution, we require

$$V(c, s) := \det(S_0 e^{N_2 L_2} S_1 e^{N_1 L_1} - \mathbb{I}) = 0.$$

This condition defines an implicit dispersion relation between wave speed c and steepness s. We then take the minimum of c with respect to s to find the minimal traveling wave speed for the linearized equation.

Figure 5 shows the numerical results from minimizing c in $V(c, s) = 0$ (blue solid curve with stars) as well as the speed from the homogenization procedure (black dashed curve). The asymptotic speed increases as the fraction of good habitat patches increases. This is to be expected. When the fraction of good patches is below the threshold that allows population persistence (see preceding section), then the speed is zero. The population does not spread but goes extinct.

The left plot in Figure 5 shows that the agreement between the homogenization and the exact solution is very good when $\beta^{\pm} \approx 1$. The left plot illustrates that the difference between the two increases as $\beta^{\pm}$ decrease. This discrepancy is related to the probability that an individual gets trapped in a (set of) patch(es); see Remark 3. Earlier we computed this probability to be $P_{\text{trap}} = (1 - \beta^{+})(1 - \beta^{-})$, which is significant when $\beta^{\pm}$ are small. We can account for this effect by multiplying the homogenized wave speed by the probability of moving on: $1 - P_{\text{trap}}$ (red curve). This correction produces a very nice fit to values of $\beta^{\pm}$ that are much smaller than 1 (e.g., the left plot for $\beta^{\pm} = 0.6$), but not for arbitrarily small values of $\beta^{\pm}$ (plots not shown).

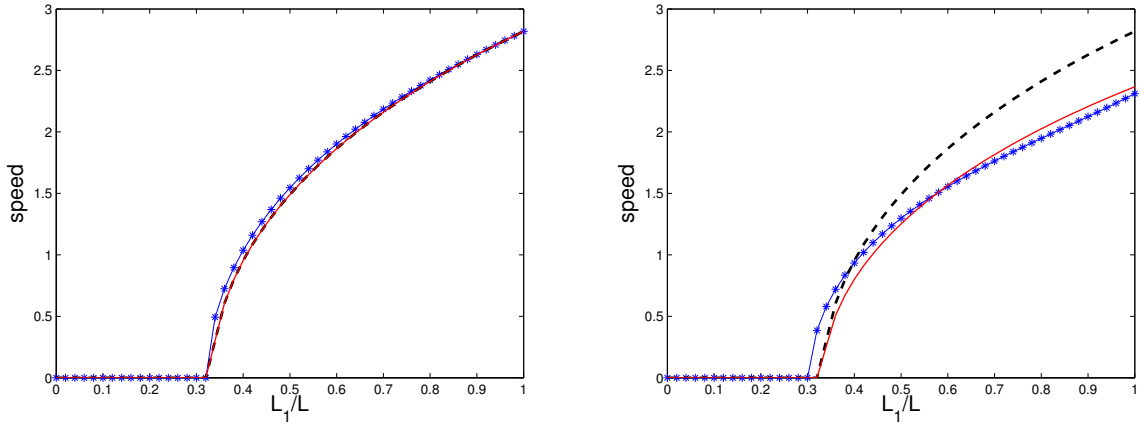

Figure 5. The speeds from homogenization (dashed) and exact dispersion relation (solid/stars) agree very well when $\beta^{+} = \beta^{-} = 1$ (left plot). When $\beta^{\pm} < 1$, the approximation becomes increasingly worse, but the rescaling with the trapping probability (solid) gives a reasonable approximation for large enough values of $\beta^{\pm}$, e.g., $\beta^{\pm} = 0.6$ (right plot). All other parameters are as in Figure 4 (top left plot) and $L = 0.5$.

6. Discussion

Most natural landscapes exhibit some level of heterogeneity at almost any scale [13]. Natural processes and human activities often create additional fragmentation of habitats into patches of different quality. Ecological theory has long recognized the importance of the extent and the distribution of patches of different quality for the persistence of biological species in such landscapes [10]. A recent modeling approach follows the landscape-ecology point of view, models landscapes as mosaics of patches of different quality and prescribes a reaction-diffusion equation for the density of reproducing and randomly moving individuals on each patch, combined with matching conditions for population density and flux across patch boundaries [1, 2, 30–32, 37, 42]. While reaction-diffusion equations are a frequently used and highly successful modeling approach for spatial ecology [4], they suffer from some of the same criticism that all diffusion models do, such as infinite propagation

speeds [9]. One alternative model formulation, based on correlated random walks, leads to systems of hyperbolic equations for individuals with a well-defined velocity [35]. The application of such models to ecology started with the seminal paper by Holmes [25] and has gained considerable momentum with the work by Hadeler, Hillen and coworkers; see, e.g., [17, 18, 21].

Our first contribution here is to derive, from basic principles, models for correlated random walks in heterogeneous landscapes, but for smooth spatial variation and for patchy landscapes as described above. We are aware of only one other attempt to model a correlated random walk with spatially dependent parameters in a physical context [11]. Their model differs from ours in that their function corresponding to our $\mu(x)$ does not appear in the turning rates. Their focus is on the effect of spatially varying and unequal turning rates.

Our second contribution is to relate the heterogeneous CRW equations to heterogeneous reaction-diffusion equations (by a parabolic scaling), as well as a homogeneous CRW (by homogenization). Then we show that the two processes commute, i.e., the homogenization of the parabolic limit is the same as the parabolic limit of the homogenization of a CRW model. In comparison to the homogenization of patchy reaction-diffusion models [42], the process for the hyperbolic system is simpler and more difficult at the same time. It is simpler in that only the zeroth and first term in the ϵ-expansion need to be considered. It is more difficult since one has a system of equations rather than a scalar model. Dealing with the interface matching conditions for the system led to some interesting questions about eigenvectors of matrices.

Our third contribution is the explicit calculation of persistence conditions and minimal speeds of periodic traveling waves for the heterogeneous CRW equations. The equations determining the minimal wave speed are only available implicitly, but this is to be expected since the corresponding parabolic theory also has this property [30, 40]. The comparison between the exact solution and the homogenized solution revealed that the accuracy of the homogenization approximation to the heterogeneous problem depends strongly on the parameters $\beta^{\pm}$. These parameters measure the probabilities that individuals continue moving in their given direction when they encounter an interface between two patches. We identified the product $(1-\beta^{+})(1-\beta^{-})$ as the probability of getting trapped, which, in effect, reduces the invasion speed by this factor. The range of movement of individuals will be limited, and with it the assumption that movement happens on a larger scale than landscape properties change. More mathematical challenges result from our model, for example, the proof of existence of solutions, the existence of periodic traveling waves, and the applicability of linear conjecture, on which we relied in our work.

Our modelling approach is based on a stochastic random walk description for an individual organism, which leads to deterministic hyperbolic and parabolic models on the population level. In some sense, this individual stochasticity vanishes in the population aggregate. Another form of stochasticity that does not vanish on the population level is a temporal change of environmental conditions in which individuals move and reproduce, for example through climatic effects. We did not include such external forcing here, which is reflected in the fact that all model parameters are constant in time. With temporally varying model parameters, one could include average seasonal variation (periodic) or random variation into the model. Other changes in environmental conditions that could influence individual movement and population dynamics include the appearance of infectious diseases or interactions with competing or predating species. Such effect could be captured by writing systems of equations for additional populations.

Acknowledgments

We would like to express our gratitude to the participants of the SQuaRE entitled "Homogenization Techniques in Ecology and Epidemiology" at the American Institute for Mathematical Sciences (AIMS) in San Jose, CA. In particular, we thank Christina Cobbold, Martha Garlick, James Powell, and Brian Yurk for much inspiration and many insightful discussions. We would also like to acknowledge our late supervisor Prof. Dr. KP. Hadeler (Universität Tübingen). During our work on this topic, we found an unpublished manuscript by Hadeler from 2003, in which he discussed an early draft of the work by Fillinger and Hongler [11]. We hope that he would have like our work presented here. Two anonymous reviewers helped us improve the presentation of our manuscript. Finally, we are grateful for support from the Natural Sciences and Engineering Research Council of Canada under the Discovery Grants Program (RGPIN-2016-04795 to FL and RGPIN-2017-04158 to TH) and a Discovery Accelerator Supplement (RGPAS-492878-2016 to FL).

Conflict of interest

All authors declare no conflicts of interest in this paper.

References

1. Y. Alqawasmeh, F. Lutscher, Movement behaviour of fish, harvesting-induced habitat degradation and the optimal size of marine reserves, *Theor. Ecol.*, **12** (2019), 453–466.
2. Y. Alqawasmeh, F. Lutscher, Persistence and spread of stage-structured populations in heterogeneous landscapes, *J. Math. Biol.*, **78** (2019), 1485–1527.
3. A. Bensoussan, J.-L. Lions, G. Papanicolaou, *Asymptotic Analysis for Periodic Structures*, Providence: AMS Chelsea Publishing, 2010.
4. R. S. Cantrell, C. Cosner, *Spatial Ecology via Reaction-Diffusion Equations*, Hoboken: Wiley, 2003.
5. B. Choi, Y.-J. Kim, Diffusion of biological organisms: Fickian and Fokker–Planck type diffusions, *SIAM J. Appl. Math.*, **79** (2019), 1501–1527.
6. J. Chung, Y. J. Kim, O. Kwong, C. W. Yoon, Biological advection and cross diffusion with parameter regimes, *AIMS Mathematics*, **4** (2020), 1721–1744.
7. Y. Dolak, T. Hillen,, Cattaneo models for chemotaxis, numerical solution and pattern formation, *J. Math. Biol.*, **46** (2003), 153–170.
8. J. P. Duncan, R. N. Rozum, J. A. Powell, K. M. Kettenring, Multi-scale methods predict invasion speeds in variable landscapes, *Theor. Ecol.*, **10** (2017), 287–303.
9. A. Einstein, Zur Theorie der Brownschen Bewegung, *Ann. Phy.*, **19** (1906), 371–381.
10. L. Fahrig, Effect of habitat fragmentation on the extinction threshold: a synthesis, *Ecol. Appl.*, **12** (2002), 346–353.
11. R. Filliger, M.-O. Hongler, Supersymmetry in random two-velocity processes, *Physica A*, **332** (2004), 141–150.

12. R. A. Fisher, The advance of advantageous genes, *Ann. Eugenics*, **7** (1937), 355–369.

13. J. F. Fryxell, Predictive modelling of patch use by terrestrial herbivores. In H.H.T. Prins and F. van Langevelde, editors, *Dynamics of Foraging Resource Ecology: Spatial and Temporal*, chapter 6A, pages 105–123. Springer, 2008.

14. M. J. Garlick, J. A. Powell, M. B. Hooten, L. R. McFarlane, Homogenization of large-scale movement models in ecology, *Bull. Math. Biol.*, **73** (2011), 2088–2108.

15. S. Goldstein, On diffusion by discontinuous movements and the telegraph equation, *Quart. J. Mech. Appl. Math.*, **4** (1951), 129–156.

16. K. P. Hadeler, Nonlinear propagation in reaction transport systems. In S. Ruan and G. Wolkowicz, editors, *Differential Equations with Applications to Biology*. The Fields Institute Lecture Series, AMS, 1998.

17. K. P. Hadeler, Reaction transport systems in biological modelling. In V. Capasso and O. Diekmann, editors, *Mathematics Inspired by Biology*, Lect. Notes Math. 1714, pages 95–150, Heidelberg, 1999. Springer Verlag.

18. K. P. Hadeler, *Topics in Mathematical Biology*, Heidelberg, Springer, 2018.

19. K. P. Hadeler, R. Illner, P. van den Driesche, A disease transport model. In G. Lumer and L. Weiss, editors, *Evolution equations and their applications in physical and life sciences*, pages 369–385, New York, 2000. Marcel Dekker.

20. T. Hillen, A Turing model with correlated random walk, *J. Math. Biol.*, **35** (1996), 49–72.

21. T. Hillen, Invariance principles for hyperbolic random walk systems, *J. Math. Ana. Appl.*, **210** (1997), 360–374.

22. T. Hillen, Hyperbolic models for chemosensitive movement, *Math. Mod. Meth. Appl. Sci.*, **12** (2002), 1007–1034.

23. T. Hillen, On the L^2-moment closure of transport equations: The general case, *Disc. Cont. Dyn. Syst. B*, **5** (2005), 299–318.

24. T. Hillen, Existence theory for correlated random walks on bounded domains, *Canad. Appl. Math. Quart.*, **18** (2010), 1–40.

25. E. E. Holmes, Are diffusion models too simple ? A comparison with telegraph models of invasion, *Am. Nat.*, **142** (1993), 779–795.

26. D. D. Joseph, L. Preziosi, Heat waves, *Rev. Mod. Phys.*, **61** (1998), 41–73.

27. M. Kac, A stochastic model related to the telegrapher's equation, *Rocky MT J. Math.*, **4** (1956), 497–509.

28. F. Lutscher, Modeling alignment and movement of animals and cells, *J. Math. Biol.*, **45** (2002), 234–260.

29. F. Lutscher, A. Stevens, Emerging patterns in a hyperbolic model for locally interacting cell systems, *J. Nonlin. Sci.*, **12** (2002), 619–640.

30. G. A. Maciel, F. Lutscher, How individual response to habitat edges affects population persistence and spatial spread, *Am. Nat.*, **182** (2013), 42–52.

31. G. A. Maciel, F. Lutscher, Allee effects and population spread in patchy landscapes, *J. Biol. Dyn.*, **9** (2015), 109–123.

32. G. A. Maciel, F. Lutscher, Movement behavior determines competitive outcome and spread rates in strongly heterogeneous landscapes, *Theor. Ecol.*, **11** (2018), 351–365.

33. J. D. Murray, *Mathematical Biology*, New York: Springer, 1989.

34. H. G. Othmer, A continuum model for coupled cells, *J. Math. Biol.*, **17** (1983), 351–369.

35. H. G. Othmer, S. R. Dunbar, W. Alt, Models of dispersal in biological systems, *J. Math. Biol.*, **26** (1988), 263–298.

36. O. Ovaskainen, S. J. Cornell,, Biased movement at a boundary and conditional occupancy times for diffusion processes, *J. Appl. Prob.*, **40** (2003), 557–580.

37. J. R. Potts, T. Hillen, M. A. Lewis,, Edge effects and the spatio-temporal scale of animal movement decisions, *Theor. Ecol.*, **9** (2015), 233–247.

38. J. Powell, N. E. Zimmermann, Multiscale analysis of active seed dispersal contributed to resolving Reid's paradox, *Ecology*, **85** (2004), 490–506.

39. H. Schwetlick, Travelling fronts for multidimensional nonlinear transport equations, *Ann. I H Poincarè (C) Ana. Nonlin.*, **17** (2000), 523–550.

40. N. Shigesada, K. Kawasaki, E. Teramoto, Traveling periodic waves in heterogeneous environments, *Theor. Popul. Biol.*, **30** (1986), 143–160.

41. P. Turchin, *Quantitative Analysis of Movement: measuring and modeling population redistribution of plants and animals*, Sunderland: Sinauer Assoc., 1998.

42. B. Yurk, C. Cobbold, Homogenization techniques for population dynamics in strongly heterogeneous landscapes, *J. Biol. Dyn.*, **12** (2018), 171–193.

43. E. Zauderer, Correlated random walks, hyperbolic systems and Fokker-Planck equations, *Math. Comupt. Model.*, **17** (1993), 43–47.

AIMS Press